Polyhedron 30 (2011) 1953–1959

Contents lists available at ScienceDirect

Polyhedron

journal homepage: www.elsevier.com/locate/poly

Synthesis, characterization and DNA-binding and DNA-photocleavage studies of two Ru(II) complexes containing two main ligands and one ancillary ligand

Jing Sun [a,b], Shuo Wu [c], Huo-Yan Chen [b], Feng Gao [b], Jie Liu [c,*], Liang-Nian Ji [b], Zong-Wan Mao [b,*]

[a] School of Pharmacy, Guangdong Medical College, Dongguan 523808, China
[b] MOE Key Laboratory of Bioinorganic and Synthetic Chemistry, School of Chemistry and Chemical Engineering, Sun Yat-Sen University, Guangzhou 510275, China
[c] Department of Chemistry, Jinan University, Guangzhou 510632, China

ARTICLE INFO

Article history:
Received 20 December 2010
Accepted 26 April 2011
Available online 18 May 2011

Keywords:
Synthesis
Ru(II) complexes
DNA-binding
Photocleavage
Density functional theory (DFT)

ABSTRACT

DNA-binding and DNA-photocleavage properties of two Ru(II) complexes, $[Ru(L^1)(dppz)_2](PF_6)_4$ (**1**) and $[Ru(L^2)(dppz)_2](PF_6)_4$ (**2**) (L^1 = 5,5′-di(1-(triethylammonio)methyl)-2,2′-dipyridyl cation; L^2 = 5,5′-di(1-(tributylammonio)methyl)-2,2′-dipyridyl cation; dppz = dipyrido[3,2-a:2′,3′-c]phenazine, have been investigated. Experimental results show that the DNA-binding affinity of complex **1** is greater than that of **2**, both complexes emit luminescence in aqueous solution, either alone or in the presence of DNA, complex **1** can bind to DNA in an intercalative mode while **2** most likely interacts with DNA in a partial intercalation fashion, and complex **2** serves as a better candidate for enantioselective binding to CT-DNA compared with **1**. Moreover, complex **1** reveals higher efficient DNA cleavage activity than **2**, during which supercoiled DNA is converted to nicked DNA with both complexes. Theoretical calculations for the two complexes have been carried out applying the density functional theory (DFT) method at the level of the B3LYP/LanL2DZ basis set. The calculated results can reasonably explain the obtained experimental trends in the DNA-binding affinities and binding constants (K_b) of these complexes.

1. Introduction

The interaction between Ru(II) polypyridine complexes and DNA has attracted much attention [1–3]. It is well established that the geometry of the DNA-binding complex plays a very important role in the interactions with nucleic acids. Thus, modification to the polypyridyl ligands allows fine tuning of the space configurations and electronic structures of Ru(II)-polypyridyl complexes. As a result, the DNA-binding behaviors of these complexes are changed. In this regard, ligands derived from 2′2-bipyridine (bpy) and 1,10-phenanthroline (phen) with various modifications have been employed to address different issues [4]. Recently, a great deal of effort has been directed toward complexes containing one main ligand and two ancillary ligands because of their stability, strong DNA affinity, photochemical properties and proven applications in several areas [5–6]. Barton and co-workers showed that the strong binding of $[Ru(L)_2(dppz)]^{2+}$ complexes (L = bpy or phen, dppz = dipyrido[3,2-*a*:2′,3′-*c*]phenazine) to DNA gave rise to a "molecular light-switch" effect, where the nearly undetectable emission from the triplet metal-to-ligand charge transfer (MLCT) excited state of $[Ru(L)_2(dppz)]^{2+}$ in water was strongly enhanced due to the intercalation of the planar dppz ligand between the base pairs of DNA [7–9]. An important characteristic of these complexes is that their main ligands possess extended and planar aromatic structures, which could insert and stack between the base pairs of double helical DNA [10–11]. Consequently, Ru(II) complexes with one ancillary ligand and two main ligands have attracted much attention [12–15]. We previously synthesized $[Ru(bpy)(pztp)_2]^{2+}$ and $[Ru(phen)(pztp)_2]^{2+}$ (pztp = 3-(pyrazin-a-yl)-as-triazino[5,6-*f*]-1,10-phenanthroline) [16], and found that both exhibited enhanced luminescence in the presence of CT-DNA and functioned as good "light switches" for DNA, though they had no extended aromatic structures. Varying the number of main ligands, on the other hand, might yield a clearer understanding of the DNA binding mechanism.

This paper mainly concerns the DNA-binding affinities of two complexes, $[Ru(L^1)(dppz)_2](PF_6)_4$ [17] and a new complex $[Ru(L^2)(dppz)_2](PF_6)_4$ (L^1 = 5,5′-di(1-(triethylammonio)methyl)-2,2′-dipyridyl cation; L^2 = 5,5′-di(1-(tributylammonio)methyl)-2,2′-dipyridyl cation), and their differences in several related properties as well as their DFT calculations resulting from slight ligand differences. The ligand system design in the two complexes may provide more understanding on how steric hindrance affects these properties. These results will hopefully be of value in further

* Corresponding authors. Tel.: +86 20 84113788, fax: +86 20 84112245.
E-mail addresses: tliuliu@jnu.edu.cn (J. Liu), cesmzw@mail.sysu.edu.cn (Z.-W. Mao).

0277-5387/$ - see front matter © 2011 Elsevier Ltd. All rights reserved.
doi:10.1016/j.poly.2011.04.047

DNA binding studies, improve efficiency in DNA recognition and cleavage by Ru(II) complexes, and lay foundations for the rational design of new photoprobes and photonucleases of DNA.

2. Materials and methods

2.1. Materials

CT-DNA was purchased from Sino-American Biotechnology Company and pBR322 DNA from Sangon Biotechnology Company, Canada. Buffer A (5.0 mM tris(hydroxymethyl)aminomethane tris-hydrochloride, 50 mM NaCl, pH 7.2) was used for absorption titration, luminescence titration, dialysis and viscosity experiments, and buffer B (50 mM Tris–HCl, 18 mM NaCl, pH 7.2) was used for DNA photocleavage experiments. The solution of CT-DNA in buffer A gave a ratio of UV absorbance of 1.8–1.9:1 at 260 and 280 nm, suggesting that the DNA was sufficiently free of protein [18]. The concentration of DNA was determined spectrophotometrically, assuming the molar absorption was 6600 $M^{-1}\,cm^{-1}$ (260 nm) [19]. The dialysis membrane was purchased from Union Carbide Co. and treated by general procedures prior to use [20]. All reagents and solvents were purchased commercially and used without further purification unless specially noted. Double distilled water was used to prepare the buffer solutions.

2.2. Physical measurements

Elemental analyses (C, H and N) were carried out with a Perkin–Elmer 240C elemental analyzer. ^{1}H NMR spectra were recorded on a Varian Mercury-plus 300 NMR spectrometer with DMSO-d_6 as the solvent and $SiMe_4$ as an internal standard at 300 MHz at room temperature. Electrospray ionization mass spectrometry (ESI-MS) was recorded on an LQC system (Finngan MAT, USA) using CH_3CN as the mobile phase. UV–Vis and emission spectra were measured on a Perkin–Elmer Lambda-850 spectrophotometer and an Ls55 spectrofluorophotometer, and circular dichroism (CD) spectra were measured on a Jasco J-810 spectropolarimeter.

2.3. Preparation of the ligands and complexes

5,5′-Dimethyl-2,2′-dipyridyl was purchased from Aldrich Chemical Co. 5,5′-Dibromomethyl-2,2′-dipyridyl, $L^1Br_2{\cdot}4H_2O$ and L^2Br_2 were synthesized and characterized according to our previous procedures [21]. 1,10-Phenanthroline-5,6-dione [22], dppz [23], *cis*-$[Ru(dppz)_2Cl_2]{\cdot}2H_2O$ [24], and complex **1** [17] were prepared and characterized according to methods reported in the literature.

2.3.1. $[Ru(L^2)(dppz)_2](PF_6)_4$ (**2**)

A solution of *cis*-$[Ru(dppz)_2Cl_2]{\cdot}2H_2O$ (0.26 g, 0.34 mmol) and L^2Br_2 (0.24 g, 0.34 mmol) in ethylene glycol (30.0 cm^3) was heated at 130 °C under the protection of argon for 6 h. In the process, the solution turned dark red. The solution was allowed to cool down to room temperature. After filtration, dropwise addition of saturated NH_4PF_6 resulted in a deep red precipitate, which was further filtered. The solid was washed with small amounts of water and diethyl ether, dried under vacuum, and then purified by column chromatography on alumina using acetonitrile as the eluent. Yield: 0.24 g (39%). *Anal.* Calc. for $C_{72}H_{84}F_{24}N_{12}P_4Ru$ (1798.44): C, 48.08; H, 4.71; N, 9.35. Found: C, 47.83; H, 4.74; N, 9.38%. ESI-MS: m/z = 1653.3 $[M-PF_6^-]^+$ (45), 754.3 $[M-2PF_6^-]^{2+}$ (100), 454.5 $[M-3PF_6^-]^{3+}$ (26). ^{1}H NMR (DMSO-d_6) δ: 9.77 (dd, 2H), 9.63 (dd, 2H), 9.10 (d, 2H), 8.53 (m, 6H), 8.30 (d, 2H), 8.20 (m, 4H), 8.10 (dd, 2H), 8.04 (d, 2H), 7.91 (s, 2H), 7.85 (dd, 2H), 4.43 (s, 4H), 2.98 (t, 12H), 1.48 (m, 12H), 1.05(m, 12H), 0.76 (t, 18H).

2.4. DNA-binding experiments

The absorption and emission titrations of the Ru(II) complexes in buffer A were performed using a fixed complex concentration, to which increments of the DNA stock solution were added. The concentration of the $[Ru(L)(dppz)_2]^{4+}$ solution was 10 μM and the volume of the complex was 3000 μL. Complex-DNA solutions were allowed to incubate for 5 min before the spectra were recorded. The titration processes were repeated several times until no change was observed in the spectra, indicating that binding saturation was achieved. Changes in the Ru(II) complex concentration due to dilution at the end of each titration were negligible.

Equilibrium dialysis was carried out in the dark and held at room temperature for 36 h with CT-DNA (1.0 mM, 5.0 mL) sealed inside a dialysis bag and a Ru(II) complex (50 μM, 10 mL) outside, the solution stirring varying with the dialysis time. For each sample, the spectrum was scanned at least three times and accumulated over a wavelength range of 200–400 nm. During the equilibrium dialysis and CD studies, a blank experiment was also carried out on the complex to ensure no obvious CD signal.

Viscosity measurements were carried out using an Ubbelohde viscometer maintained at a constant temperature of 30.0 ± 0.1 °C in a thermostatic bath. DNA samples with an approximate average length of 200 base pairs were prepared by sonication in order to minimize complexities arising from DNA flexibility [25]. The flow time was measured with a digital stopwatch. Each sample was measured three times and an average flow time was calculated and used. Data were presented as $(\eta/\eta^0)^{1/3}$ versus binding ratio ([Ru]/[DNA]) [26], where η was the viscosity of DNA in the presence of the complex and η^0 was the viscosity of DNA alone.

2.5. DNA photocleavage experiments

During the gel electrophoresis experiments, supercoiled pBR322 DNA (0.10 μg) was treated with a Ru(II) complex in buffer B, and the solution was subsequently irradiated at room temperature with a UV lamp (365 nm, 10 W) for 60 min. The samples were analyzed by electrophoresis for 3 h at 60 V on 1.0% agarose gel in TBE buffer (89 mM tris–borate acid, 2.0 mM EDTA, pH 8.3). The gel was stained with EB (3,8-diamino-5-ethyl-6-phenylphenanthridinium bromide, 1.0 μg mL^{-1}) and photographed with an Alpha Innotech IS-5500 fluorescence chemiluminescence and visible imaging system.

2.6. Theoretical section

Each complex is formed from a Ru(II) ion, two main ligands (dppz) and one ancillary ligand (L^1 or L^2). Full geometry optimization computations were performed applying the DFT-B3LYP method [27–30] and LanL2DZ basis set [31,32], and assuming the singlet state for the complexes [33]. All computations were performed with the GAUSSIAN03 quantum chemistry program-package [34]. In order to vividly depict the details of the frontier molecular orbital interactions, stereographs of some related frontier molecular orbitals of the complexes were drawn with the MOLDEN v4.4 program [35] based on the DFT calculational results.

3. Results and discussion

3.1. Synthesis

Similar to that of complex **1**, the synthetic route to complex **2** is summarized in Scheme 1. Each synthetic step involved here was quite straightforward and provided a moderate yield of the desired product in a pure form. The products were characterized by ele-

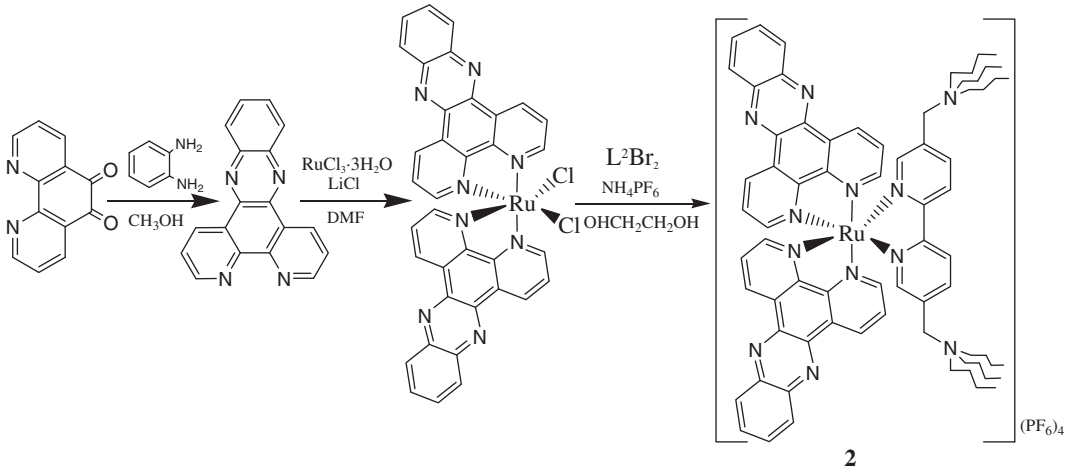

Scheme 1. Synthetic route to complex **2**.

mental analysis, ^{1}H NMR and electrospray ionisation mass spectra (ESI-MS).

3.2. Absorption spectra

Electronic absorption spectroscopy serves as the most common means to study the interactions between metal complexes and DNA [18]. A complex binding to DNA through intercalation usually results in hypochromism and bathchromism, due primarily to the intercalation mode involving a strong stacking interaction between an aromatic chromophore and the base pairs of DNA. It is generally accepted that the extent of the hypochromism in a UV–Vis band is consistent with the strength of interaction [36–38]. The absorption spectra of complexes **1** and **2** in the absence and presence of CT-DNA are compared in Fig. 1, and other related data are listed in Table 1.

The absorption spectra of complexes **1** and **2** exhibit similar characters, i.e., there are three bands with comparable intensity ranging between 250 and 550 nm. Two intra-ligand (IL) transitions in the UV region, at 282 and 360 nm, are observed for complexes **1** and **2**, respectively. There is also a metal-to-ligand charge transfer (^{1}MLCT) in the visible region around 450 nm, likely arising from Ru(II) ($d\pi$) to dppz [39].

With an increase in concentration of DNA, all the absorption bands of the complexes display clear hypochromism, and a red shift is observed in the MLCT band of the complexes. The hypochromism (H%) of the MLCT bands in complexes **1** and **2**, defined as $H\% = 100\%\ (A_{free} - A_{bound})/A_{free}$, is determined to be about (11.18 ± 0.05)% and (11.04 ± 0.05)%, respectively. In order to compare the DNA-binding affinities of the two complexes quantitatively, their intrinsic binding constants K_b to DNA are obtained from monitoring the changes in the MLCT absorbance for both complexes according to Eq. (1) [39–43], where [DNA] is the DNA concentration in nucleotides, ε_a is the extinction coefficient (A_{abs}/[M]) observed for the MLCT absorption band at a given DNA concentration, and ε_f and ε_b are, respectively, the extinction coefficients for the free Ru(II) complex and Ru(II) complex in the fully bound form. K_b is the equilibrium binding constant in M^{-1}, C_t is the total Ru(II) complex concentration and s is the binding site size. Eq. (1) is applied to absorption titration data of non-cooperative metallointercalators binding to CT-DNA.

$$(\varepsilon_a - \varepsilon_f)/(\varepsilon_b - \varepsilon_f) = (b - (b^2 - 2K_b^2 C_t[\mathrm{DNA}]/s)^{1/2}/2K_b C_t \quad (1a)$$

$$b = 1 + K_b C_t + K_b[\mathrm{DNA}]/2s \quad (1b)$$

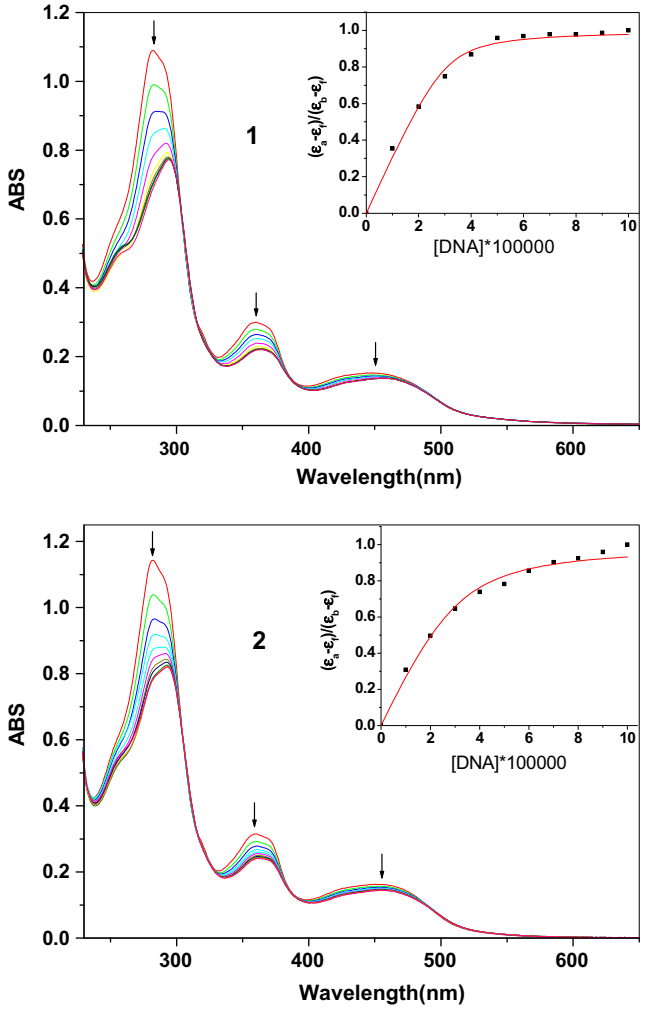

Fig. 1. Absorption spectra of complexes **1** and **2** in buffer A in the presence of increasing amounts of CT-DNA. [Ru] = 10 μM, [DNA] = 0–100 μM from top to bottom. Arrows indicate the change in absorbance upon increasing the DNA concentration. Inset: plot of $(\varepsilon_a - \varepsilon_f)/(\varepsilon_b - \varepsilon_f)$ versus [DNA] and the non-linear fit for the titration of DNA to Ru(II) complexes.

From the decay of the absorbance, the intrinsic binding constants K_b of complexes **1** and **2** are measured to be $(1.9 \pm 0.6) \times 10^6\ M^{-1}$ and $(0.58 \pm 0.2) \times 10^6\ M^{-1}$, respectively. The

Table 1
Absorption spectra (λ_{max}/nm) and DNA-binding constants K_b ($\times 10^6\ M^{-1}$) of complexes **1** and **2**.

Complex	λ_{max}(free)	λ_{max}(bound)	$\Delta\lambda$/nm	H/(%)	$K_b/10^6\ M^{-1}$	s
1	444	459	15	11.18	1.9 ± 0.6	1.5 ± 0.1
	360	364	4	26.56		
	282	294	12	29.30		
2	453	455	2	11.04	0.58 ± 0.2	1.5 ± 0.2
	360	365	5	23.75		
	282	293	11	28.27		

binding constant K_b of complex **1** is greater than that of **2**, revealing a stronger DNA-binding affinity of **1** compared to **2**. Since the two complexes have the same main ligand, the difference comes mostly from the ancillary ligands, where the methyl group in complex **1** gives less steric hindrance than the ethyl group in **2**. The two complexes in the current study are found to have K_b values larger than $[Ru(phen)(dicnq)_2]^{2+}$ ($K_b = 3.0 \times 10^4\ M^{-1}$, dicnq = 6,7-dicyanodipyrido[2,2-d:2′3′-f]quinoxaline) [12], $[Ru(bpy)(pztp)_2]^{2+}$ and $[Ru(phen)(pztp)_2]^{2+}$ ($K_b = 1.4 \times 10^4\ M^{-1}$ and $K_b = 4.8 \times 10^4\ M^{-1}$) [16], but smaller K_b values than complexes having extended-aromatic structures, such as $[Ru(bpy)(pp[2,3]p)_2]^{2+}$ and $[Ru(phen)(pp[2,3]p)_2]^{2+}$ ($K_b = 3.08 \times 10^6\ M^{-1}$ and $K_b = 6.53 \times 10^6\ M^{-1}$, pp[2,3]p = pyrido[2′3′:5,6]pyrazino[2,3-*f*][1,10]phenanthroline) [13]. This is mainly because the extended-aromatic structures of the dppz ligand increase the action between the complexes and DNA, but the steric hindrance of quaternary ammonium cation weakens the effect. Although a charge increase in the ligands gives no affinity enhancement between the complexes and DNA, the above results indicate that the ancillary ligands (L^1 or L^2) directly affect the DNA-binding affinity.

3.3. Luminescence studies

The results of the luminescence titration for the two complexes with DNA are shown in Fig. 2. Upon excitation using wavelengths of 447 and 453 nm for complexes **1** and **2**, respectively, both complexes exhibit luminescence in buffer A with a maximum wavelength of about 630 nm in the presence of CT-DNA. The luminescence intensity of the complexes increases with the increase in CT-DNA concentration and reaches a maximum at a ratio of [DNA]/[Ru] of about 18:1. We can also derive the binding constants of the two complexes interacting with DNA from the emission spectra using the luminescence titration method [44]. The binding data obtained from the emission spectra were fitted using the McGhee and Von Hippel equation [45] to acquire the binding parameters. The intrinsic binding constants K_b of $6.4(\pm0.4) \times 10^6\ M^{-1}$ for complex **1** and $2.0(\pm0.6) \times 10^6\ M^{-1}$ for complex **2** were determined. Comparing these values with those obtained from absorption spectra, although the binding constants obtained from the fluorescence with the McGhee–von Hippel method are different from those obtained from absorption, both sets of binding constants show that complex **1** binds to DNA more avidly than complex **2**.

3.4. Enantioselective binding studies

According to the proposed binding mode [18,46], the Δ-enantiomer of the complex, a right-handed propeller-like structure, will display a greater affinity for the right-handed CT-DNA helix than the Λ-enantiomer, owing to the more appropriate steric matching. The enantiospecific binding of complexes to DNA can be examined clearly from circular dichroism spectra, with the presence of CD signals indicative of enrichment in the enantiomer less favorably binding to DNA in dialysate.

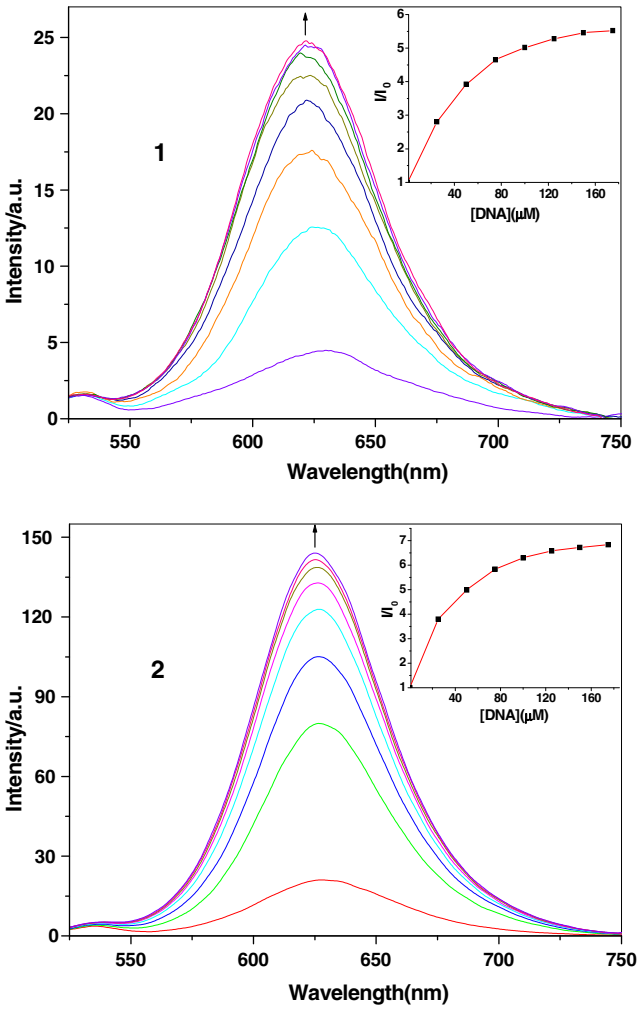

Fig. 2. Emission spectra of complexes **1** and **2** in buffer A in the presence of increasing amounts of CT-DNA, [Ru] = 10 μM, [DNA] = 0–175 μM. Arrow shows the emission intensity changes upon increasing the DNA concentration. I_0 is the fluorescence intensity in the absence of DNA, I is the observed fluorescence emission intensity at the given DNA concentration.

The CD spectra in the UV region 250–50 nm are shown in Fig. 3 for complexes **1** and **2** after their racemic solutions are dialyzed against CT-DNA. As shown in the spectra, complex **2** exhibits a stronger CD signal than **1**. Although neither of the complexes is resolved into pure enantiomers, and it cannot be determined which enantiomer preferentially binds to DNA for each complex, it is rather certain that both of the complexes interact with CT-DNA enantioselectively, while complex **2** is a better candidate for enantioselectively binding to CT-DNA.

3.5. Viscosity studies

Optical photophysical probes provide necessary, albeit not sufficient, insight to support a binding model. Hydrodynamic measurements, i.e. viscosity and sedimentation, that are sensitive to length changes are regarded as the least ambiguous and most critical tests to a binding model in solution in the absence of crystallographic structural data [44,47]. A classical intercalation model usually results in lengthening of the DNA helix as base pairs are separated to accommodate the bound ligand, leading to an increase in the DNA viscosity. In contrast, semi-intercalation of a ligand could bend or kink the DNA helix, and thus reduce its effective length and, concomitantly, its viscosity. Moreover, certain

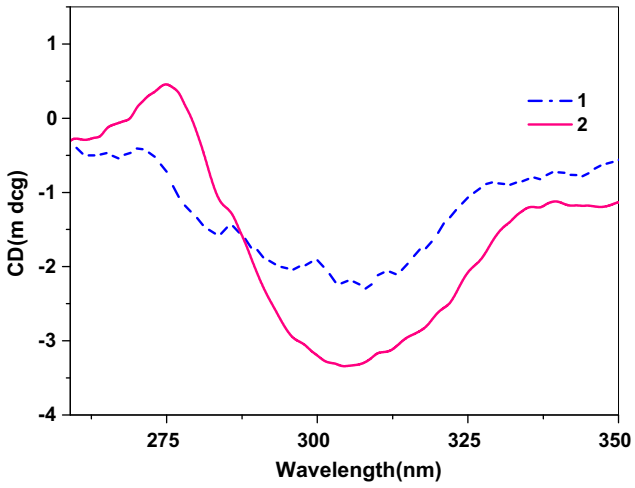

Fig. 3. CD spectra of complexes **1** and **2** in buffer A in the presence of CT-DNA, [Ru] = 50 μM, [DNA] = 1.0 mM.

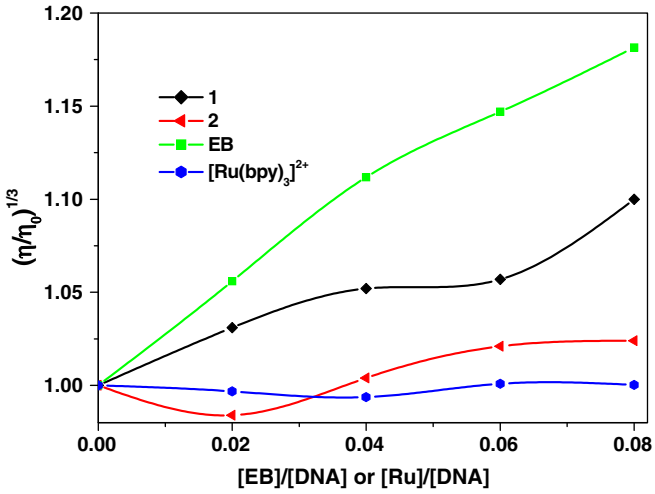

Fig. 4. Effects of increasing amounts of complexes **1** (♦), **2** (▼), EB (■) and $Ru(bpy)_3^{2+}$ (●) on the relative viscosities of CT-DNA at 30.0 ± 0.1 °C, [DNA] = 0.5 mM, r = [Ru]/[DNA].

complexes, such as $[Ru(bpy)_3]^{2+}$, which interact with DNA in an electrostatic binding mode, have no influence on the DNA viscosity [48].

The changes in the relative viscosity of rod-like CT-DNA in the presence of $[Ru(L)(dppz)_2]^{4+}$ (L^1 or L^2), EB and $[Ru(bpy)_3]^{2+}$ are shown in Fig. 4. EB, a well-known DNA intercalator, can strongly raise the relative viscosity by lengthening the DNA double helix through intercalation. On the contrary, $[Ru(bpy)_3]^{2+}$, which binds to DNA in an electrostatic mode, exerts essentially no effect on the DNA viscosity. As revealed in Fig. 4, upon increasing the amounts of complex **1**, the relative viscosity of DNA increases similarly to the behavior of EB. This observation suggests that the principal mode of DNA binding by **1** involves base-pair intercalation, with one dppz ligand intercalating into the base pairs and

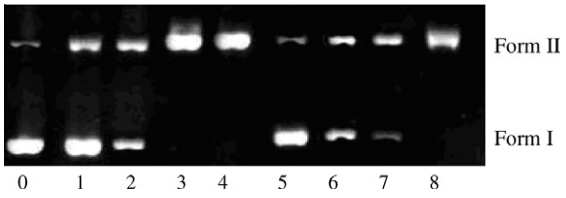

Fig. 5. Photocleavage of supercoiled pBR322 DNA in the presence of complexes **1** (lane 1–4) and **2** (lane 5–8) in 2, 4, 6, and 8 μM, respectively. All lanes are under irradiation at 365 nm for 60 min.

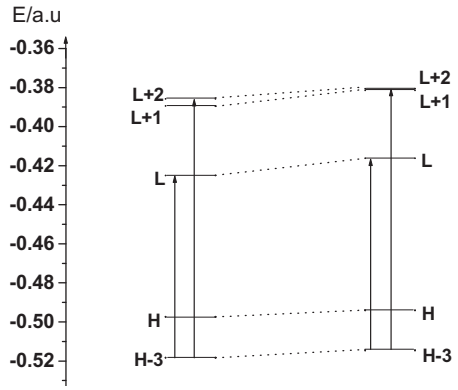

Fig. 6. Schematic diagram of the energies and related energy transitions of complexes **1** and **2** (L = LUMO, H = HOMO).

the other dppz ligand being left outside the helix [16]. In contrast, complex **2** can decrease the viscosity of DNA at low binding ratios (r < 0.04) and gradually increase it upon further molar ratio (r) increase. The results suggest that the binding modes of complexes **1** and **2** differ markedly, and while **1** can intercalate between DNA base-pairs, complex **2** most likely interacts with DNA in a partially intercalating mode [49].

3.6. Photocleavage of pBR 322 DNA by Ru(II) complexes

There is substantial and continuing interest in DNA endonucleolytic cleavage reactions that are activated with metal ions [50,51]. The cleavage reaction on plasmid DNA can be conveniently monitored by agarose gel electrophoresis. When circular plasmid DNA is subjected to electrophoresis, relatively fast migration will be observed for the intact supercoil form (form I). If scission occurs on one strand (nicking), the supercoil will relax to generate a slower-moving open circular form (form II). If both strands are cleaved, a linear form (form III) that migrates between forms I and II will be generated. Fig. 5 shows the gel electrophoresis separation of pBR322 DNA after incubation with complex **1** or **2** and irradiation at 365 nm. Only a little DNA cleavage is observed for a control study, where there is no metal complex (lane 0). For complex **1**, at a concentration of 2 μM (line 1), approximately half of the supercoiled plasmid has been converted to the nicked form; at a concentration of 6 μM (line 3), it can promote the complete conversion of DNA from Form I to Form II. However, complex **2** only promotes the complete conversion of DNA from Form I to

Table 2
Some frontier molecular orbital energies (ε_i/atomic unit) of the complexes (1 atomic unit = 27.21 eV).

Complex	HOMO − 8	HOMO − 7	HOMO − 6	HOMO − 5	HOMO − 4	HOMO − 3	HOMO − 2	HOMO − 1	HOMO	LUMO	LUMO + 1	LUMO + 2
1	−0.53475	−0.53463	−0.52606	−0.52315	−0.51989	−0.51833	−0.51820	−0.49747	−0.49734	−0.42509	−0.38944	−0.38582
2	−0.52915	−0.52829	−0.51958	−0.51925	−0.51557	−0.51466	−0.51439	−0.49411	−0.49398	−0.41622	−0.38138	−0.38058

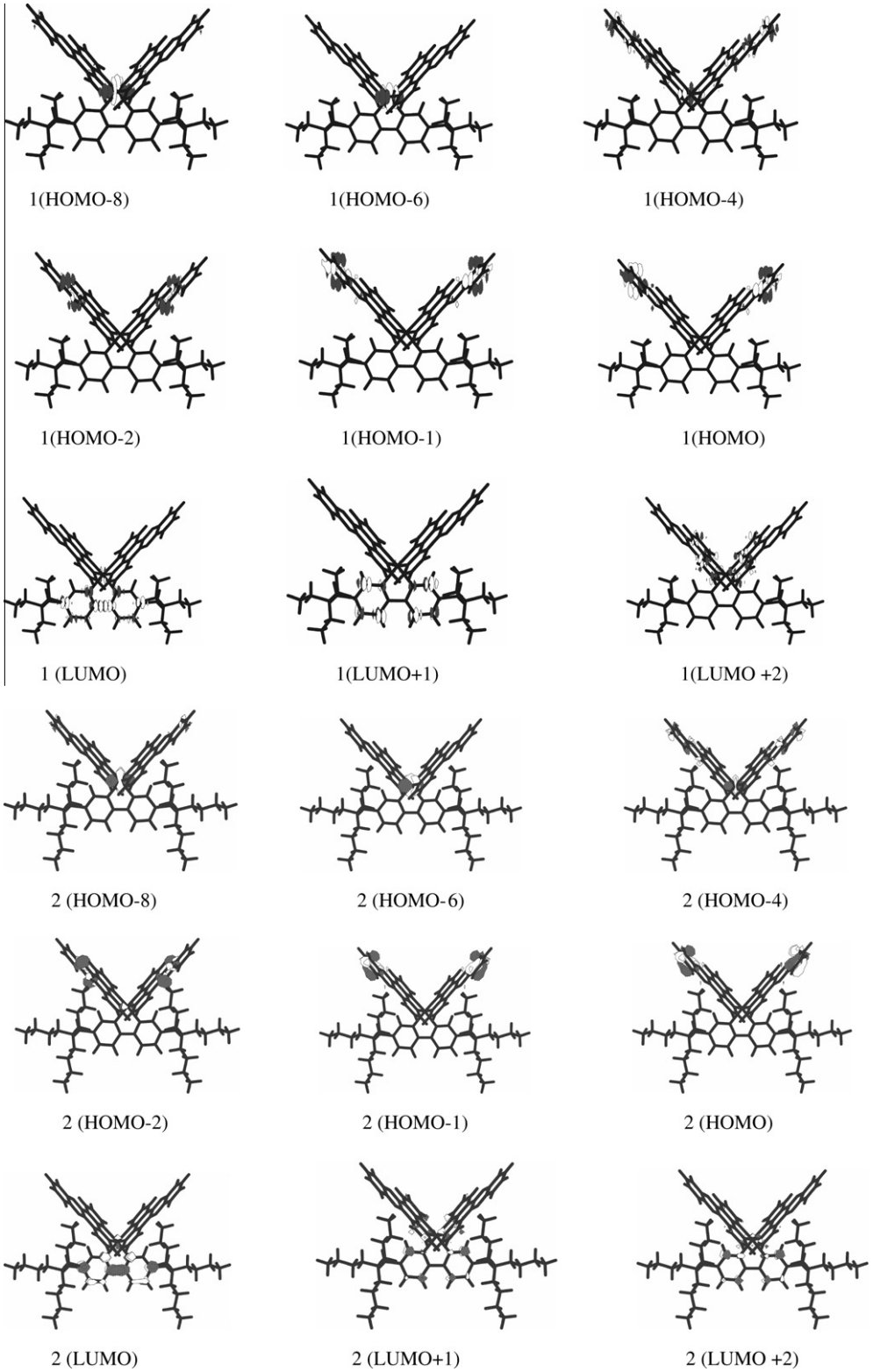

Fig. 7. Contour plots of some related frontier molecular orbital stereographs of complexes **1** and **2** using the DFT method at the B3LYP/LanL2DZ level.

Form II at a concentration of 8 μM. The difference in DNA-cleavage ability may originate from the different DNA-binding affinity.

3.7. Theoretical explanation of DNA binding behavior

The different DNA-binding behavior of the two title complexes can be reasonably explained by DFT calculations and frontier molecular orbital theory [52–54]. Some frontier MO energies are listed in Table 2. A schematic diagram of the energies and related ^{1}MLCT transitions are shown in Fig. 6, and the related orbital stereographs of the two complexes are presented in Fig. 7.

As is well-established, there are π–π stacking interactions in the DNA-binding of these complexes upon intercalation (or partial intercalation) [16], and many theoretical studies [55,56] have also

shown that the DNA molecule is an electron-donor and the intercalated complex is an electron-acceptor. Therefore, the factors affecting the DNA-binding affinities of the complex can usually be considered from the planarity and plane area of the main ligand, and the energy and population of the lowest unoccupied molecular orbital (LUMO, and even LUMO + x, x = 1, 2, 3) of the complex molecule. A lower LUMO (and LUMO + x) energy of the complex easily accepts electrons from the HOMO (and HOMO − x) of the DNA base-pairs and the more population of the LUMO (and LUMO + x) on the intercalative ligand is advantageous to the orbital interaction between the LUMO (and LUMO + x) of the complex and the HOMO (and HOMO − x) of DNA according to frontier molecular orbital theory [53,54].

Since complexes **1** and **2** have the same main ligand, dppz, the planarity area of the main ligand in each case is equal. The energy and population of the lowest unoccupied molecular orbital (LUMO, even and LUMO + x) of the molecule can be considered as the main factor affecting the DNA-binding affinities of the complexes. In fact, we can see that the related frontier MO contour plots of the two title complexes are very alike from Fig. 7, the LUMO (and LUMO + x) of complexes **1** and **2** are mostly distributed on the ancillary ligands, and thus their LUMO (and LUMO + x) should play an important role in accepting electrons from base pairs of DNA. From Table 2 and Fig. 6, we can clearly see that the order of the energies of the LUMO (and LUMO + x) of the two complexes are $\varepsilon_L(\mathbf{2}) > \varepsilon_L(\mathbf{1})$ and ε_{L+x} (**2**) > ε_{L+x} (**1**). Since lower energies of the LUMO and LUMO + x must be advantageous to accepting the electrons of the HOMO of DNA in the π–π interaction based on the frontier MO theory, the experimental trend in the DNA-binding constants (K_b), i.e. $K_b(\mathbf{1}) > K_b(\mathbf{2})$, can be reasonably explained.

4. Conclusion

In this paper, we studied the DNA-binding and photocleavage properties of two Ru(II) complexes with two main ligands and one ancillary ligand. The results indicate that complex **1** has a greater DNA affinity than **2**. Moreover, complex **1** can strongly bind to CT-DNA through intercalation, while **2** binds to DNA in a partial intercalative mode. When irradiated at 365 nm, the two Ru(II) complexes efficiently photocleave plasmid pBR 322 DNA. Applying DFT/TDDFT calculations and frontier molecular orbital theory, the trend in DNA-binding affinities, can be reasonably explained.

Acknowledgements

This work was supported by the National Natural Science Foundation of China (Nos. 30770494, 20725103, 20831006 and 20821001), the Guangdong Provincial Natural Science Foundation (No. 9351027501000003), National Basic Research Program of China (973 Program No. 2007CB815306) and the Doctoral Program of Guangdong Medical College (B2009003).

Appendix A. Supplementary data

^{1}H NMR spectra of dppz, complex **2** and their assignments (Figs. S1, S2, S3) are included as supplementary materials. Supplementary data associated with this article can be found, in the online version, at doi:10.1016/j.poly.2011.04.047.

References

[1] K.E. Erkkila, D.T. Odom, J.K. Barton, Chem. Rev. 99 (1999) 2777.
[2] L.N. Ji, X.H. Zou, J.G. Liu, Coord. Chem. Rev. 216–217 (2001) 513.
[3] J.G. Vos, J.M. Kelly, J. Chem. Soc., Dalton Trans. (2006) 4869.
[4] Y. Xiong, L.N. Ji, Coord. Chem. Rev. 185–186 (1999) 711.
[5] C. Metcalfe, J.A. Thomas, Chem. Soc. Rev. 32 (2003) 215.
[6] M.J. Hannon, Chem. Soc. Rev. 36 (2007) 280.
[7] A.E. Friedman, J.C. Chambron, J.P. Sauvage, N.J. Turro, J.K. Barton, J. Am. Chem. Soc. 112 (1990) 4960.
[8] A.E. Friedman, C.V. Kumar, N.J. Turro, J.K. Barton, Nucl. Acids Res. 19 (1991) 2595.
[9] R.M. Hartshorn, J.K. Barton, J. Am. Chem. Soc. 114 (1992) 5919.
[10] S.P. Foxon, C. Metcalfe, H. Adams, M. Webb, J.A. Thomas, Inorg. Chem. 46 (2007) 409.
[11] V. Rajendiran, M. Murali, E. Suresh, S. Sinha, K. Somasundaram, M. Palaniandavar, J. Chem. Soc., Dalton Trans. (2008) 148.
[12] A. Ambroise, B.G. Maiya, Inorg. Chem. 39 (2000) 4264.
[13] B.Y. Wu, L.H. Gao, Z.M. Duan, K.Z. Wang, J. Inorg. Biochem. 99 (2005) 1685.
[14] N. Nickita, M.J. Belousoff, A.I. Bhatt, A.M. Bond, G.B. Deacon, G. Gasser, L. Spiccia, Inorg. Chem. 46 (2007) 8638.
[15] J. Sun, S. Wu, Y. Han, J. Liu, L.N. Ji, Z.W. Mao, Inorg. Chem. Commun. 11 (2008) 1382.
[16] X.H. Zou, B.H. Ye, H. Li, Q.L. Zhang, H. Chao, J.G. Liu, L.N. Ji, X.Y. Li, J. Biol. Inorg. Chem. 6 (2001) 143.
[17] J. Sun, Y. An, L. Zhang, Y. Han, H.Y. Chen, Y.J. Wang, Z.W. Mao, L.N. Ji, J. Inorg. Biochem. 105 (2011) 149.
[18] J.K. Barton, A.T. Danishefsky, G.M. Goldberg, J. Am. Chem. Soc. 106 (1984) 2172.
[19] J. Marmur, J. Mol. Biol. 3 (1961) 208.
[20] M.E. Reichmann, S.A. Rice, C.A. Thomas, P. Doty, J. Am. Chem. Soc. 76 (1954) 3047.
[21] Y. An, Y.Y. Lin, H. Wang, H.Z. Sun, M.L. Tong, L.N. Ji, Z.W. Mao, J. Chem. Soc., Dalton Trans. (2006) 2066.
[22] W. Paw, R. Eisenberg, Inorg. Chem. 36 (1997) 2287.
[23] C.M. Dupureur, J.K. Barton, Inorg. Chem. 36 (1997) 33.
[24] G. Albano, P. Belser, C. Daul, Inorg. Chem. 40 (2001) 1408.
[25] J.B. Chaires, N. Dattagupta, D.M. Crothers, Biochemistry 21 (1982) 3933.
[26] G. Cohen, H. Eisenberg, Biopolymers 8 (1969) 45.
[27] P. Hohenberg, W. Kohn, Phys. Rev. B 136 (1964) 864.
[28] A.D. Becke, J. Chem. Phys. 98 (1993) 1372.
[29] A. Görling, Phys. Rev. A 54 (1996) 3912.
[30] J.B. Foresman, A.E. Frisch, In Exploring Chemistry with Electronic Structure Methods, second ed., Gaussian Inc., PA, Pittsburgh, 1996.
[31] P.J. Hay, W.R. Wadt, J. Chem. Phys. 82 (1985) 270.
[32] P.J. Hay, W.R. Wadt, J. Chem. Phys. 82 (1985) 299.
[33] A. Juris, V. Balzani, F. Barigelletti, S. Campagna, P. Belser, A.V. Zelewsky, Coord. Chem. Rev. 84 (1988) 85.
[34] M.J. Frisch, G.W. Trucks, H.B. Schlegel, G.E. Scuseria, M.A. Robb, J.R. Cheeseman, J.A. Montgomery, T.V. Jr., K.N. Kudin, J.C. Burant, J.M. Millam, S.S. Iyengar, J. Tomasi, V. Barone, B. Mennucci, M. Cossi, G. Scalmani, N. Rega, G.A. Petersson, H. Nakatsuji, M. Hada, M. Ehara, K. Toyota, R. Fukuda, J. Hasegawa, M. Ishida, T. Nakajima, Y. Honda, O. Kitao, H. Nakai, M. Klene, X. Li, J.E. Knox, H.P. Hratchian, J.B. Cross, V. Bakken, C. Adamo, J. Jaramillo, R. Gomperts, R.E. Stratmann, O. Yazyev, A.J. Austin, R. Cammi, C. Pomelli, J.W. Ochterski, P.Y. Ayala, K. Morokuma, G.A. Voth, P. Salvador, J.J. Dannenberg, V.G. Zakrzewski, S. Dapprich, A.D. Daniels, M.C. Strain, O. Farkas, D.K. Malick, A.D. Rabuck, K. Raghavachari, J.B. Foresman, J.V. Ortiz, Q. Cui, A.G. Baboul, S. Clifford, J. Cioslowski, B.B. Stefanov, G. Liu, A. Liashenko, P. Piskorz, I. Komaromi, R.L. Martin, D.J. Fox, T. Keith, M.A. Al-Laham, C.Y. Peng, A. Nanayakkara, M. Challacombe, P.M.W. Gill, B. Johnson, W. Chen, M.W. Wong, C. Gonzalez, J.A. Pople, Gaussian 03, Revision D.01,Gaussian, Inc., Wallingford CT, 2005.
[35] G. Schaftenaar, J.H. Noordik, J. Comput.-Aided Mol. Des. 14 (2000) 123.
[36] A.M. Pyle, J.P. Rehmann, R. Meshoyrer, C.V. Kumar, N.J. Turro, J.K. Barton, J. Am. Chem. Soc. 111 (1989) 3051.
[37] L.F. Tan, X.L. Liang, X.H. Liu, J. Inorg. Biochem. 103 (2009) 441.
[38] J. Talib, D.G. Harman, C.T. Dillon, J. Aldrich-Wright, J.L. Becka, S.F. Ralph, J. Chem. Soc., Dalton Trans. (2009) 504.
[39] R.B. Nair, E.S. Teng, S.L. Kirkland, C.J. Murphy, Inorg. Chem. 37 (1998) 139.
[40] L.M. Chen, J. Liu, J.C. Chen, C.P. Tan, S. Shi, K.C. Zheng, L.N. Ji, J. Inorg. Biochem. 102 (2008) 330.
[41] M.T. Carter, M. Rodriguez, A.J. Bard, J. Am. Chem. Soc. 111 (1989) 8901.
[42] P. Uma Maheswari, M. Palaniandavar, J. Inorg. Biochem. 98 (2004) 219.
[43] S. Shi, Xi.T. Geng, J. Zhao, T.M. Yao, C.R. Wang, D.J. Yang, L.F. Zheng, L.N. Ji, Biochimie 92 (2010) 370.
[44] S. Satyanarayana, J.C. Dabrowiak, J.B. Chaires, Biochemistry 31 (1992) 9319.
[45] J.D. McGhee, P.H. Von Hippel, J. Mol. Biol. 86 (1974) 469.
[46] C.V. Kumar, J.K. Barton, N.J. Turro, J. Am. Chem. Soc. 107 (1985) 5518.
[47] S. Satyanarayana, J.C. Dabrowiak, J.B. Chaires, Biochemistry 32 (1993) 2573.
[48] J.G. Liu, B.H. Ye, H. Li, Q.X. Zhen, L.N. Ji, Y.H. Fu, J. Inorg. Biochem. 76 (1999) 265.
[49] S. Shi, J. Liu, J. Li, K.C. Zheng, C.P. Tan, L.M. Chen, L.N. Ji, J. Chem. Soc., Dalton Trans. (2005) 2038.
[50] D.S. Sigman, Acc. Chem. Res. 19 (1986) 180.
[51] B. Armitage, Chem. Rev. 98 (1998) 1171.
[52] K. Fukui, T. Yonezawa, H. Shingu, J. Chem. Phys. 20 (1952) 722.
[53] G. Klopman, J. Am. Chem. Soc. 90 (1968) 223.
[54] I. Fleming, Frontier Orbital and Organic Chemical Reaction, Wiley, New York, 1976.
[55] N. Kurita, K. Kobayashi, Comput. Chem. 24 (2000) 351.
[56] D. Reha, M. Kabelac, F. Ryjacek, J. Sponer, J.E. Sponer, M. Elstner, S. Suhai, P. Hobza, J. Am. Chem. Soc. 124 (2002) 3366.